Acta Geologica Sinica (English Edition), 2020, 94(5): 1728–1730

Research Advances

Transient Fluvial Incision in the Central Segment of the Lancang River Orogenic Belt, Yunnan Province, SW China

SHI Xiaohui[1, 2, *], LI Tingting[3], PEI Lixin[1], WANG Qingtao[1], HUI Bo[1] and CHENG Chao[1]

[1] *State Key Laboratory of Continental Dynamics, Department of Geology, Northwest University, Xi'an 710069, China*
[2] *Key Laboratory of Deep-Earth Dynamics of Ministry of Natural Resources, Institute of Geology, Chinese Academy of Geological Sciences, Beijing 100037, China*
[3] *Chengji Middle School, Jingning County, Pingliang, Gansu 743409, China*

Citation: Shi et al., 2020. Transient Fluvial Incision in the Central Segment of the Lancang River Orogenic Belt, Yunnan Province, SW China. Acta Geologica Sinica (English Edition), 94(5): 1728–1730. DOI: 10.1111/1755-6724.14589

Objective

Geomorphology has played a central role in the study of active orogenic belts. Extensive tectonic deformation associated with the collision of the Indian and Eurasian plates has occurred in the southeastern margin of the Tibetan Plateau, particularly along the Lancang River Orogenic Belt (LROB) and the Lancang River Fault. Therefore, the landscape evolution of the LROB has significant implications for understanding the tectonic process of intracontinental mountain building and plateau growth. In this study, we used digital elevation models (DEMs) to extract longitudinal profile information on the fluvial systems of the central segment of the LROB. The paleolongitudinal profile developed on the low-relief landscape was reconstructed and the data were used to estimate the amount of surface uplift in the central segment of the LROB. The main purpose of this study was to detect the channel response to tectonic deformation in the southeastern Tibetan Plateau.

Methods

In a wide variety of natural settings, fluvial topographic data exhibit a power-law relationship between the local channel slope (S) and upstream drainage area (A):

$$S = k_s A^{-\theta}, \quad (1)$$

where θ is referred to as the concavity index and is related to the area and gradient, and k_s is the steepness index, which is considered to be a function of the uplift rate and erosion coefficient.

We used 30-m-resolution (1 arc second) DEM data to extract longitudinal profiles. The morphometric analyses were carried out using ArcGIS to generate the hydrographic network; MATLAB scripts were used to extract and analyze channel profiles and to calculate channel steepness indices. We chose an average moving window of 250 m to remove spikes and to smooth channel profiles and used an equal vertical interval of 12.192 m to calculate channel gradients. The normalized steepness index (k_{sn}) was calculated using a reference concavity (θ_{ref}) value of 0.45. In addition, to estimate the amount of incision recorded by the transient channel profile, the paleolongitudinal profile was reconstructed by using the assumption of steady-state channel gradients based on the relict channel profile. The amount of incision should be equal to the magnitude of surface uplift.

Results

The topographic metrics of the 19 channels of the central segment of LROB are summarized in Appendix 1. Longitudinal profiles for the 19 channels were extracted. Eighteen of these channels have a "slope-break" knickpoint (Fig. 1a). Knickpoints are associated with slope changes in the chi–elevation plots and delineate channel network portions with different values of channel steepness (Fig. 1b). The channel segments upstream of knickpoints exhibit low steepness indices (mean k_{sn} = 47.65 ± 4.46), whereas downstream channel segments are relatively steeper (mean k_{sn} = 190.94 ± 4.56) (Fig. 1c). Most of these knickpoints are distributed within a narrow elevation range of 2200–2400 m (Fig. 1b). The longitudinal profile of a representative channel (channel 5) shows that the knickpoint separates the low-gradient upstream channel reach with a k_{sn} value of 22 $m^{0.9}$ from the steeper downstream channel reach with a k_{sn} value of 223 $m^{0.9}$ (Fig. 1d). The low-gradient upstream channel reach represents the relict landscape. The paleolongitudinal profile projection of channel 5 indicates that it has a total incision of ~900–1100 m (Fig. 1d). The majority of river mouths occur in a narrow window of elevation between 1000 and 1200 m (Fig. 1b). Therefore, the amount of incision of channel 5 can represent the average incision of these 19 channels and the amount should be equal to the magnitude of surface uplift.

Conclusions

This study of the response of bedrock channel profiles to tectonic activity in the central segment of the LROB yielded the following conclusions.

(1) Longitudinal profile analysis revealed that the landscape evolution of the central segment of the LROB is in a transient state. The landscape upstream of knickpoints represents the relict landscape, whereas the downstream

* Corresponding author. E-mail: shixhok@163.com

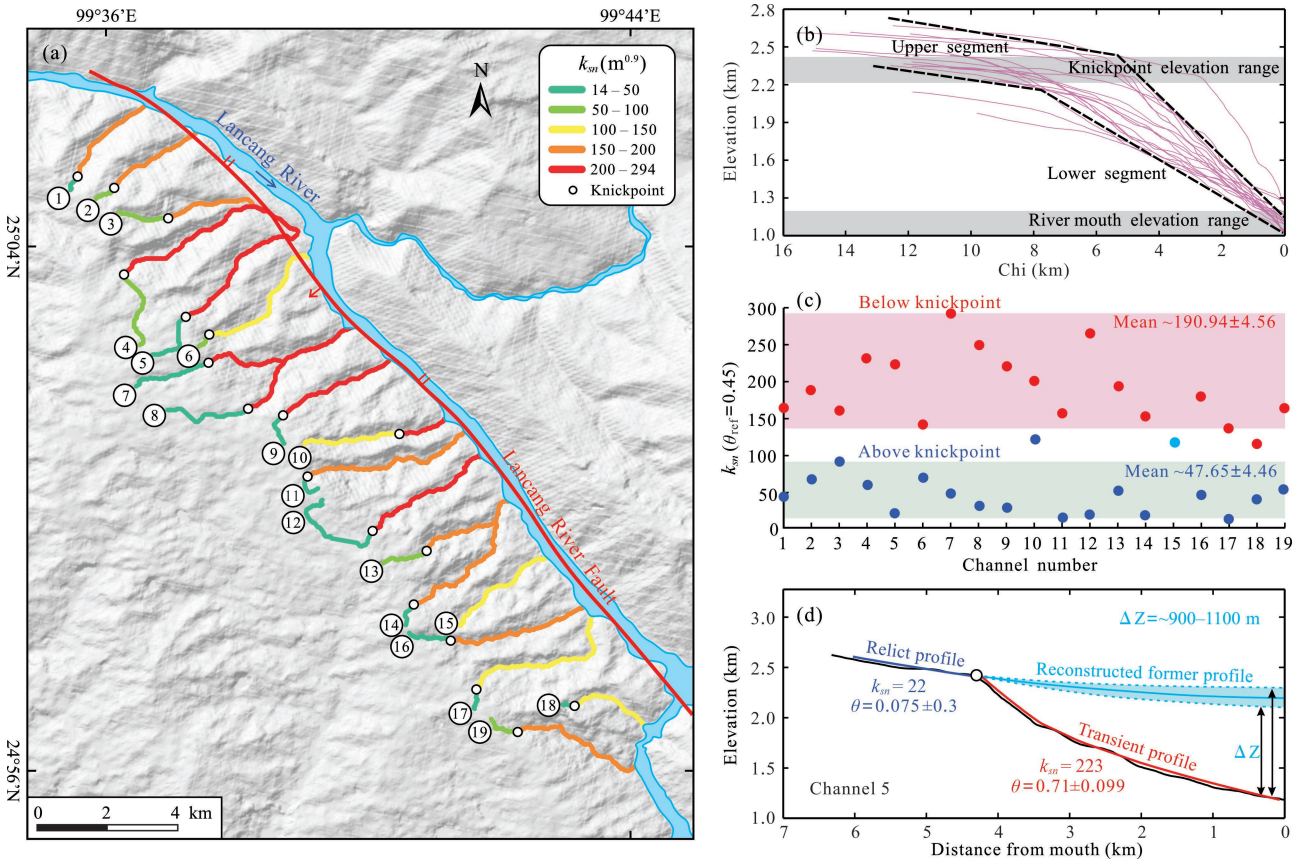

Fig. 1. Results of channel longitudinal profile analysis in the central segment of the Lancang River Orogenic Belt. (a) Channel profiles in the central segment of the Lancang River Orogenic Belt color-coded by steepness index (k_{sn}). Knickpoints are shown as white circles. (b) Chi–elevation plots for the 19 longitudinal profiles. "Chi (km)" represents the integral of the catchment area over the distance. (c) Channel steepness index for the 19 longitudinal profiles (blue – channel segments upstream of knickpoints; red – channel segments downstream of knickpoints; light blue – channel without knickpoint). (d) Example of present longitudinal profile and paleolongitudinal profile reconstruction of the study area.

area is an adjusting landscape.

(2) The paleochannel reconstruction indicated that the central segment of the LROB has experienced a total surface uplift of ~900–1100 m since knickpoint initiation. This uplift can be attributed to the southeastward growth of the Tibetan Plateau.

Acknowledgements

This work was supported by the National Natural Science Foundation of China (Grant: 41902208), China Postdoctoral Science Foundation (Grant: 2020M673623XB), Natural Science Foundation of Shaanxi Province, China (Grant: 2020JQ-583), and Open Research Fund of Key Laboratory of Deep-Earth Dynamics of Ministry of Natural Resources, Institute of Geology, Chinese Academy of Geological Sciences (Grant: J1901). We thank Lucy Muir, PhD, from Liwen Bianji, Edanz Editing China (www.liwenbianji.cn/ac), for editing the English text of a draft of this manuscript. We are also grateful to the anonymous referee for the helpful comments and constructive suggestions which substantially improved this work.

Appendix 1 Topographic characteristics of stream profiles in the study area

No. [a]	Length (km)	A_{min} [b] (m^2)	A_{max} [b] (m^2)	θ±2δ	k_{sn}±2δ (θ_{ref}=0.45)	R^2	Comments
1	0.39	1.1×10^4	1.2×10^5	0.072±0.071	47.2±3.6	0.29	Upper reach
1	3.20	1.2×10^5	3.4×10^6	0.3±0.043	162±3.0	0.71	Lower reach
2	0.57	3.5×10^4	2.1×10^5	0.15±0.14	66.2±1.9	0.24	Upper reach
2	3.03	2.1×10^5	4.0×10^6	0.37±0.085	187±3.0	0.51	Lower reach
3	1.32	2.5×10^4	1.3×10^6	0.14±0.081	94.3±5.2	0.28	Upper reach
3	2.55	1.3×10^6	3.7×10^6	1.3±0.29	161±9.0	0.64	Lower reach
4	2.34	5.1×10^4	3.0×10^6	0.19±0.14	57.8±2.7	0.25	Upper reach
4	5.68	3.0×10^6	1.4×10^7	1±0.24	231±6.0	0.45	Lower reach
5	1.68	4.2×10^4	8.6×10^5	0.075±0.3	22±2.1	0.023	Upper reach
5	4.25	8.6×10^5	5.3×10^6	0.71±0.099	223±4.0	0.67	Lower reach
6	0.47	2.5×10^4	2.9×10^5	0.18±0.15	71.5±2.2	0.27	Upper reach
6	4.78	2.9×10^5	5.4×10^6	0.43±0.085	144±3.0	0.52	Lower reach
7	2.35	2.7×10^5	3.4×10^6	0.29±0.23	48.3±1.9	0.27	Upper reach
7	2.46	3.4×10^6	5.3×10^6	-0.67±0.61	294±6.0	0.073	Lower reach
8	2.41	1.9×10^4	1.2×10^6	-0.033±0.23	33±6.6	0.004	Upper reach
8	4.10	1.2×10^6	7.1×10^6	0.49±0.09	250±3.0	0.54	Lower reach
9	0.95	8.1×10^4	5.3×10^5	-0.78±0.46	27.2±10.1	0.7	Upper reach
9	3.30	5.3×10^5	4.1×10^6	0.29±0.087	219±4.0	0.32	Lower reach
10	3.04	1.4×10^5	2.3×10^6	0.44±0.12	124±2.0	0.47	Upper reach
10	2.01	2.3×10^6	2.6×10^7	0.69±0.29	200±8.0	0.38	Lower reach
11	0.84	1.2×10^4	2.4×10^5	0.074±0.52	15±2.8	0.016	Upper reach
11	5.83	2.4×10^5	5.9×10^6	0.35±0.064	153±1.0	0.52	Lower reach
12	3.41	4.9×10^4	2.6×10^6	0.35±0.30	21.6±1.3	0.31	Upper reach
12	4.65	2.6×10^6	7.5×10^6	0.072±0.24	264±6.0	0.0036	Lower reach
13	1.42	2.9×10^4	9.3×10^5	0.16±0.22	50.8±9.5	0.11	Upper reach
13	2.43	9.3×10^5	3.2×10^6	1±0.22	195±7.0	0.61	Lower reach
14	0.70	2.0×10^4	2.8×10^5	0.25±0.41	18.5±2.7	0.28	Upper reach
14	5.51	2.8×10^5	8.2×10^6	0.38±0.07	154±2.0	0.53	Lower reach
15	4.02	4.3×10^4	4.2×10^6	0.20±0.06	117±3.0	0.37	
16	1.36	2.4×10^4	1.1×10^6	0.19±0.096	49±2.7	0.46	Upper reach
16	5.12	1.1×10^6	7.0×10^6	0.31±0.15	181±3.0	0.17	Lower reach
17	0.55	2.0×10^4	2.3×10^5	-0.93±1.70	14.9±14.3	0.5	Upper reach
17	6.33	2.3×10^5	7.4×10^6	0.41±0.054	137±6.0	0.7	Lower reach
18	0.99	1.6×10^4	1.4×10^5	0.77±0.26	38.9±4.2	0.87	Upper reach
18	4.65	1.4×10^5	3.7×10^6	0.16±0.097	114±4.0	0.16	Lower reach
19	0.99	1.3×10^5	5.2×10^5	-0.66±0.35	57.5±4.4	0.5	Upper reach
19	4.65	5.2×10^5	3.8×10^8	0.071±0.13	168±4.0	0.013	Lower reach

[a] See Fig. 1a for stream locations.

[b] A_{min} and A_{max} refer to the minimum and maximum drainage areas, respectively, considered in the regression.